

## •COMMUNICATIONS•

SPECIAL TOPIC: Electrocatalysis &amp; Energy Science

November 2020 Vol.63 No.11: 1557–1562  
<https://doi.org/10.1007/s11426-020-9808-6>

## Intrinsically high efficiency sodium metal anode

Yifang Zhang<sup>1,2</sup>, Qiuwei Shi<sup>1</sup>, Yiren Zhong<sup>1</sup> & Hailiang Wang<sup>1\*</sup><sup>1</sup>Department of Chemistry and Energy Sciences Institute, Yale University, West Haven, CT 06516, USA;<sup>2</sup>Joint School of National University of Singapore and Tianjin University, International Campus of Tianjin University, Binhai New City, Fuzhou 350207, China

Received June 1, 2020; accepted June 28, 2020; published online August 18, 2020

Efficient plating/stripping of Na metal is critical to stable operation of any rechargeable Na metal battery. However, it is often overlooked or misunderstood in electrochemical measurements using thick Na electrodes with large excess of Na reserves. Herein, we report two crucial aspects, which have generally been ignored in previous studies, in the development of more practical capacity-controlled Na metal electrodes that can be efficiently cycled at 100% depth. We find that common carbonate electrolytes induce severe side reaction and highly irreversible Na plating/stripping, whereas ether electrolytes without any additive support thick Na metal electrodes operating at a high average Coulombic efficiency of 99.6% for over 300 cycles. We further show that to realize such high efficiency in thin Na metal electrodes, it is necessary to ensure strong adhesion between the thin Na layer and the Cu current collector, which we solve by introducing an Au interlayer. The resulting transferable thin Na metal electrodes enable high-energy-density, high-efficiency and reasonably stable-cycling Na||Na<sub>3</sub>V<sub>2</sub>(PO<sub>4</sub>)<sub>3</sub> batteries.

**sodium metal battery, electrolyte, Coulombic efficiency, deep cycling**

**Citation:** Zhang Y, Shi Q, Zhong Y, Wang H. Intrinsically high efficiency sodium metal anode. *Sci China Chem*, 2020, 63: 1557–1562, <https://doi.org/10.1007/s11426-020-9808-6>

The low cost and high abundance of Na resources has brought Na-based batteries on the front burner of future energy storage technologies [1–4]. Resembling Li metal for Li batteries, Na metal, with its high specific capacity (1,164 mAh g<sup>-1</sup>) and low redox potential (-2.714 V vs. SHE (standard hydrogen electrode)), is the optimal anode material for Na batteries except for its side reaction and dendrite formation tendency causing poor reversibility in electrochemical plating/stripping and hence a short cycle life [5–9]. While many approaches have been taken to improve the stability of Na metal electrodes, most of these studies were based on thick Na electrodes that are shallowly cycled (e.g., <10% of total capacity) [6]. This is not ideal for application because the large excess amount of Na significantly dilutes the energy density of the battery. This also disconnects cycling performance from the efficiency of Na plating/stri-

ping, which is a critical measure of electrode reversibility, because the excess Na can compensate any loss of active Na during cycling. Consequently, in most studies the Na metal electrode fails before all the available Na is consumed, and hence the observed cycle life is not directly related to the Coulombic efficiency (CE) of the electrode [10]. Therefore, it is necessary to study thin Na metal electrodes with controlled capacities under deep-cycling conditions. It was only recently that thin and deep-cycling Li metal electrodes were explored [11–13]. Such studies for Na metal electrodes remain limited [14,15].

In this work, we develop a Na metal electrode that can be cycled at 100% depth with a high CE. In doing so, we find that Na metal electrodes suffer from substantial side reaction and highly irreversible plating/stripping in common carbonate-based electrolytes, whereas in ether-based electrolytes they demonstrate high reversibility without the need for extra modification/protection. While Na||Cu cells using 1 M

\*Corresponding author (email: [hailiang.wang@yale.edu](mailto:hailiang.wang@yale.edu))

$\text{NaPF}_6$  in tetraethylene glycol dimethyl ether (TEGDME) as electrolyte exhibit CEs as high as 99.6%, the Cu electrode with electrochemically deposited Na cannot be reused in another cell because of the fragile contact between the Na and Cu layers. Using a thin Au interlayer allows us to solve this problem and enables transferable Na metal electrodes with controlled capacities that can be cycled at 100% depth with CEs up to 99.48%. This high performance is further confirmed in  $\text{Na}||\text{Na}_3\text{V}_2(\text{PO}_4)_3$  full cells.

Despite earlier reports suggesting that ether electrolytes give higher CE than carbonate electrolytes for Na metal electrodes [8], recent studies still frequently use symmetric  $\text{Na}||\text{Na}$  cells operating with carbonate electrolytes to evaluate the performance [9,16–24]. Therefore, we first examined two commonly used carbonate electrolytes, namely 1 M  $\text{NaClO}_4$  in propylene carbonate (PC) and 1 M  $\text{NaPF}_6$  in ethylene carbonate (EC)-diethyl carbonate (DEC) mixture (1:1, v/v) [5]. The  $\text{Na}||\text{Na}$  cells both showed non-smooth charging-discharging voltage profiles with kinks and average over-

potentials over 200 mV at the current of  $0.5 \text{ mA cm}^{-2}$  (Figure S1(a, b), [Supporting Information online](#)), which indicates severe loss of active Na and high resistance [25]. The cells failed with symptoms of substantially increased overpotentials and voltage fluctuations after only 160 h of cycling (Figure 1(a, b)).  $\text{Na}||\text{Cu}$  cell measurements showed very low CEs of about 10% (Figure 1(d), and Figures S2, S3), confirming that the Na plating/stripping process is highly irreversible. When 5 wt% of fluoroethylene carbonate (FEC), which is a commonly used additive for improving alkaline metal electrode performance in carbonate electrolytes [26,27], was blended in the PC and EC-DEC electrolytes, both the kinetics and cycle life were improved. The  $\text{Na}||\text{Na}$  cells achieved about 300 h of cycling under  $0.5 \text{ mA cm}^{-2}$ - $1 \text{ mAh cm}^{-2}$  current-capacity conditions (Figure 1(a, b)). Overpotentials were reduced to  $\sim 50$  mV with smooth voltage profiles recorded (Figure S1(c, d)). However, the Na plating/stripping process in these FEC-containing carbonate electrolytes is still highly inefficient, with CEs of

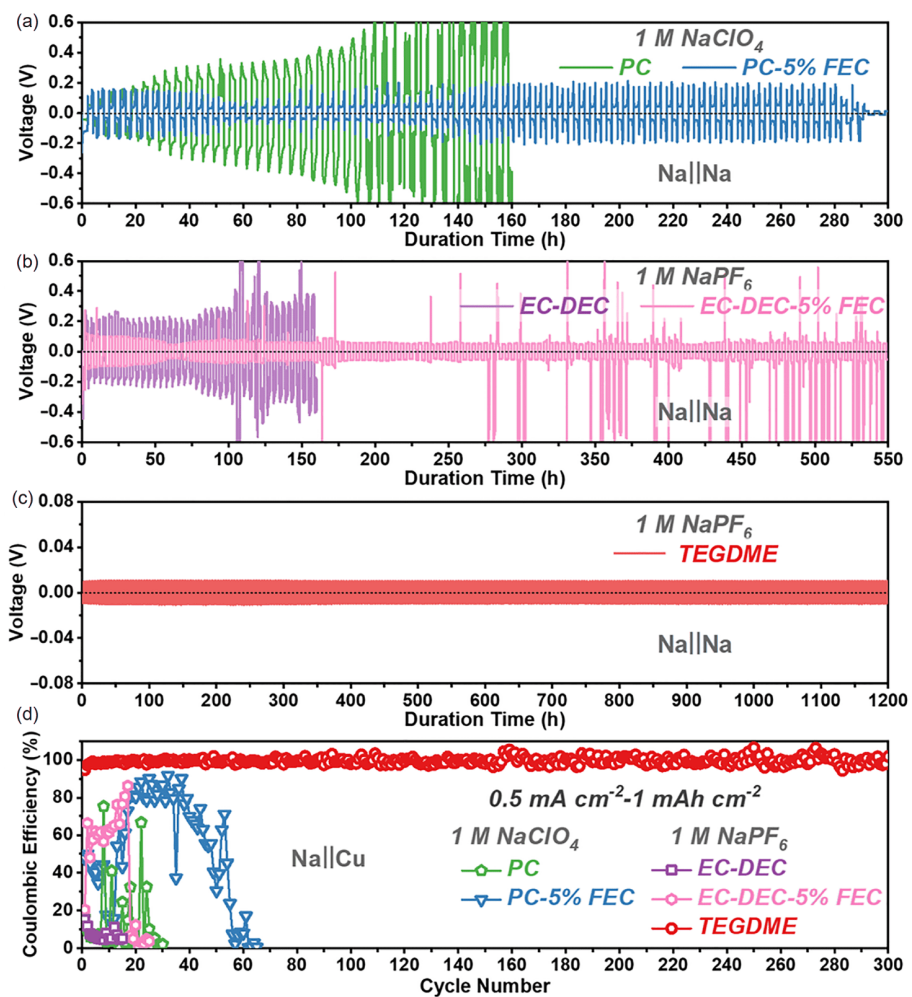


**Figure 1** (a–c) Charging-discharging voltage profiles of  $\text{Na}||\text{Na}$  symmetric cells with different electrolytes under  $0.5 \text{ mA cm}^{-2}$ - $1 \text{ mAh cm}^{-2}$  conditions: (a) 1 M  $\text{NaClO}_4$  in PC or PC with 5% FEC; (b) 1 M  $\text{NaPF}_6$  in EC-DEC or EC-DEC with 5% FEC; (c) 1 M  $\text{NaPF}_6$  in TEGDME. (d) CEs of  $\text{Na}||\text{Cu}$  cells with different electrolytes under  $0.5 \text{ mA cm}^{-2}$ - $1 \text{ mAh cm}^{-2}$  conditions (color online).

~50% as revealed by the Na||Cu measurements (Figure 1(d), and Figures S4, S5). Taking all these results together, we can conclude that Na metal electrodes are not compatible with the common carbonate electrolytes likely due to both electrolyte decomposition and “dead” Na formation [10,25,28,29]. In fact, all of the carbonate cells measured in this study lost more than  $4 \text{ mAh cm}^{-2}$  of electrochemically active Na in less than 10 cycles (Figure S6), which precludes them from being useful in any real rechargeable battery. Note that these problems are not readily evident from typical Na||Na cell measurements where smooth voltage profiles and hundreds of cycles may be observed.

We found ether-based electrolytes work well for Na metal electrodes. Using 1 M NaPF<sub>6</sub> in TEGDME as electrolyte, both Na||Na and Na||Cu cells showed high reversibility and cycling stability. The overpotentials of the Na||Na cell were only ~10 mV at  $0.5 \text{ mA cm}^{-2}$  and remained unchanged over 1,200 h of continuous cycling at the capacity of  $1 \text{ mAh cm}^{-2}$  (Figure 1(c), and Figure S1(e, f)). The Na||Cu cell was operated for 300 cycles with a high average CE of 99.6% (Figure 1(d)) and much smaller overpotentials and more stable voltage profiles than those using carbonate electrolytes (Figures S7, S8). Consequently, the consumption of active Na was greatly suppressed to only  $1.22 \text{ mAh cm}^{-2}$  for the 300 cycles (Figure S6). We note that the Na||Na and Na||Cu cells could have been cycled even longer because of the stable Na plating/stripping behavior. However, such cycling would be less meaningful because the extended cycle life is sustained by the huge excess of Na in the electrode, which is different from the real battery scenario where the Na metal anode is of a limited capacity and is cycled deeply.

To this end, we performed an experiment in which we first

electrochemically deposited a controlled amount of Na on a Cu current collector and then disassembled the Na||Cu cell to study the Na@Cu electrode in a different cell (see details in the [Supporting Information online](#)). When paired with a clean Cu electrode and cycled in the voltage range of  $-1$ – $1 \text{ V}$  to plate/stripping all the active Na, *i.e.*, at 100% depth (inset of Figure 2(a)), the Na@Cu electrode delivered only half of the expected capacity ( $0.497 \text{ mAh cm}^{-2}$  vs. the pre-deposited  $1 \text{ mAh cm}^{-2}$ ) in the first stripping step, which further dropped to ~ $0.1 \text{ mAh cm}^{-2}$  in the second cycle (Figure 2(a)). Considering the high CE of the Na||Cu cell using the same electrolyte, the capacity loss was most likely introduced by the cell disassembly-electrode transfer-cell assembly process. However, it is highly unlikely the deposited Na would deteriorate chemically during the transfer process since this step was handled with care in Ar atmosphere. Therefore, we believe the poor adhesion of Na to Cu, as reflected in the photograph shown in Figure 2(b), is responsible for Na detachment from the current collector and hence the capacity fade. The fluctuating voltage profiles and rapidly increasing overpotentials also reveal the poor contact between the thin layer of Na and the underlying Cu substrate (Figure 2(c)).

To solve this issue and investigate the intrinsic performance of capacity-controlled thin Na metal electrodes, we pre-coated the Cu current collector with a thin layer (50 nm) of Au, which can alloy with Na and improve the adhesion as shown by previous studies [30,31]. Electrochemically deposited Na on the Au@Cu electrode shows a uniform and flat surface (Figure 3(a)). When paired with a Au@Cu electrode (Figure 3(b)), the Na@Au@Cu electrode (initial capacity  $2 \text{ mAh cm}^{-2}$ ) was plated/stripped at  $0.5 \text{ mA cm}^{-2}$  and 100% depth for 150 cycles. The average CE (CE<sub>avg</sub>) of the Na

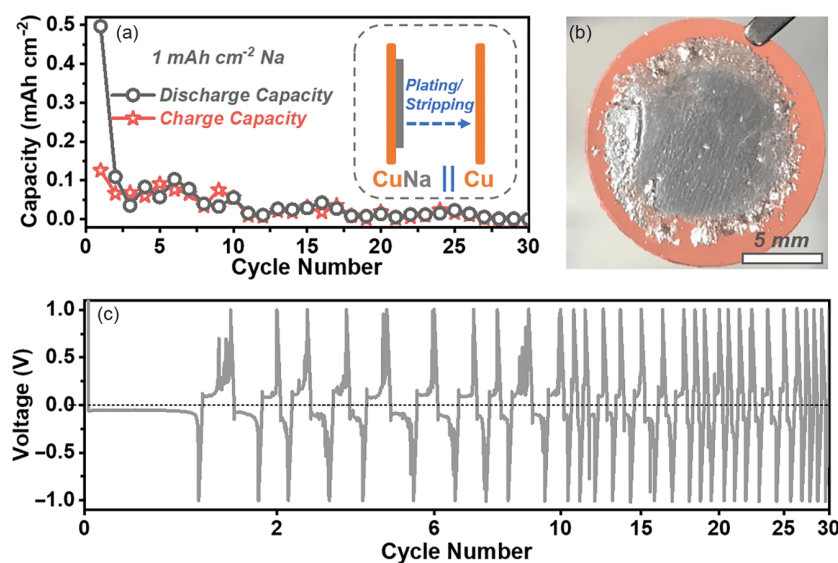


**Figure 2** (a) Capacity retention of Na@Cu||Cu cell cycled at  $0.5 \text{ mA cm}^{-2}$  with  $1 \text{ mAh cm}^{-2}$  of pre-deposited Na. Inset shows the cell configuration; (b) photograph of a Cu electrode with  $1 \text{ mAh cm}^{-2}$  of electrochemically deposited Na metal; (c) charging-discharging voltage profiles of the Na@Cu||Cu cell (color online).

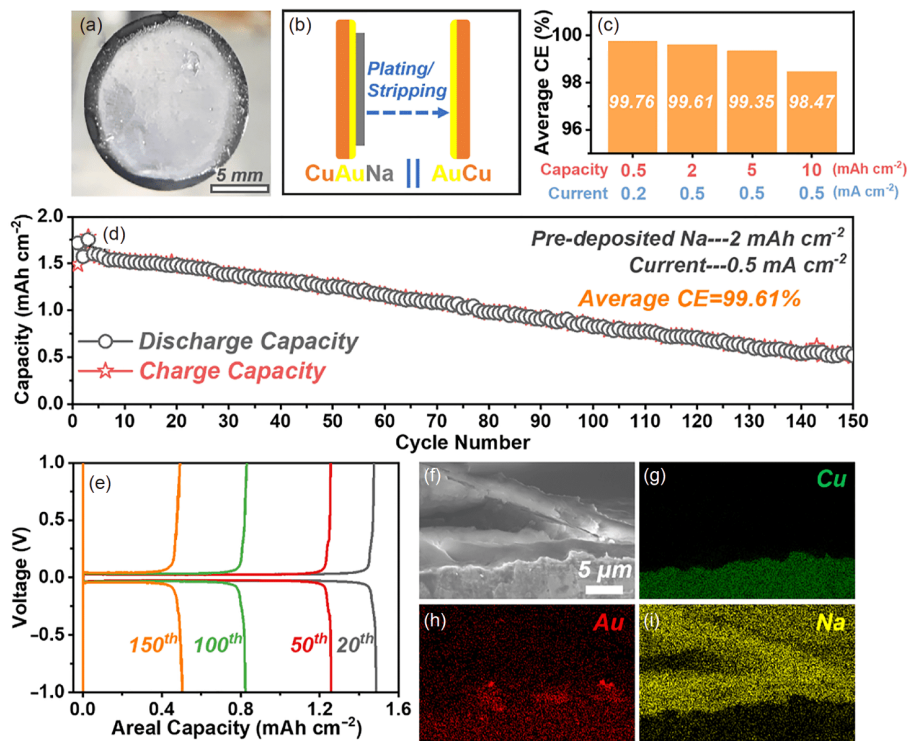


**Figure 3** (a) Photograph of an Au@Cu electrode with  $1 \text{ mAh cm}^{-2}$  of electrochemically deposited Na metal; (b) Na@Au@Cu||Au@Cu cell configuration; (c) average CE of Na@Au@Cu||Au@Cu cells cycled at different current densities with different pre-deposited Na capacities; (d) capacity retention and (e) selected charging-discharging voltage profiles of Na@Au@Cu||Au@Cu cell cycled at  $0.5 \text{ mA cm}^{-2}$  with  $2 \text{ mAh cm}^{-2}$  of pre-deposited Na; (f-i) SEM imaging and EDS mapping of Na@Au@Cu electrode with  $2 \text{ mAh cm}^{-2}$  of pre-deposited Na after five cycles at  $0.5 \text{ mA cm}^{-2}$ . Partial overlapping of Au and Cu signals is likely caused by sample preparation (color online).

plating/stripping process was calculated from the capacity decaying behavior using the following equation:

$$\text{CE}_{\text{avg.}} = \sqrt[2(n-1)]{\frac{C_n}{C_1}},$$

where  $n$  is the cycle number and  $C_n$  is the measured capacity of that cycle. Since Na plating/stripping occurs at both electrodes in any given cycle, the root index is  $2(n-1)$  in the equation. Considering the CE may be capacity-dependent, we calculated the average value based on a  $C_n$  that is  $\sim 30\%$  of  $C_1$ . The obtained average CE values for different current-capacity conditions are plotted in Figure 3(c). At  $0.5 \text{ mA cm}^{-2}$ - $2 \text{ mAh cm}^{-2}$ , 99.61% is achieved, comparable to those measured using Na||Cu cells. The CE decreases slightly with increasing amount of initially deposited Na (Figure 3(c, d) and Figures S9, S10). Although the capacity of the Na@Au@Cu electrode gradually decreased over the 150 cycles, the overpotentials of the charging/discharging voltage plateaus remained unchanged (Figure 3(e)), which indicates that the good contact between Na and Au@Cu was sustained during the cycling. Consistently, scanning electron microscopy (SEM) imaging and energy dispersive X-ray spectroscopy (EDS) mapping showed that the Au interlayer remained in place after cycling (Figure 3(f-i)).

Control experiments show that coating Au on the Cu

current collector does not alter the electrochemical performance of the Na||Cu cell with the TEGDME electrolyte, nor does it solve the low reversibility problem for the carbonate electrolytes (Figures S11, S12). Therefore, the major role of the Au interlayer is to improve the contact between Na and Cu, and hence to enable the preparation and stable cycling of the thin Na metal electrode. The adhesion improvement is likely related to the formation of a Na-Au alloy phase. The Na||Au@Cu cell manifests a small platform at  $\sim 0.25 \text{ V}$  vs.  $\text{Na}^+/\text{Na}$  in its Na stripping (from the Na@Au@Cu electrode) voltage profile (Figure S12(c)), which corresponds to Na removal from the  $\text{Na}_2\text{Au}$  alloy phase [31]. The observation that this dealloying process appears at the end of the stripping process again confirms that the Au interlayer is underneath the deposited Na. Interestingly, we found that the thin Na cell requires Au coating on both Cu current collectors to function well (Figures S13, S14), whereas the Na||Cu cell does not need that (Figure 1(d)). The origin to this difference is not fully understood at this stage, but may be related to the elasticity of the thick Na electrode of the Na||Cu cell, which can help maintain a pressure on the Na@Cu electrode in the cell and ensure a good contact between the Na and Cu. Benefits of mechanical pressure to Li metal anodes have been reported [32–34].

Real batteries are always fabricated with the amounts of

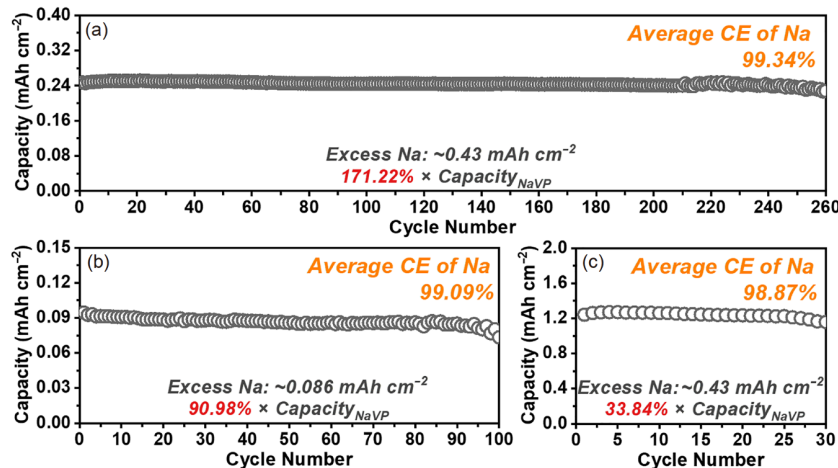


**Figure 4** Cycling performance of  $\text{Na}@\text{Au}@\text{Cu}||\text{Na}_3\text{V}_2(\text{PO}_4)_3$  cells with different amounts of excess Na at  $0.2 \text{ mA cm}^{-2}$ . (a)  $\sim 0.43 \text{ mAh cm}^{-2}$  of excess Na paired with  $\sim 0.25 \text{ mAh cm}^{-2}$  of  $\text{Na}_3\text{V}_2(\text{PO}_4)_3$ ; (b)  $\sim 0.086 \text{ mAh cm}^{-2}$  of excess Na paired with  $\sim 0.094 \text{ mAh cm}^{-2}$  of  $\text{Na}_3\text{V}_2(\text{PO}_4)_3$ ; (c)  $\sim 0.43 \text{ mAh cm}^{-2}$  of excess Na paired with  $\sim 1.27 \text{ mAh cm}^{-2}$  of  $\text{Na}_3\text{V}_2(\text{PO}_4)_3$  (color online).

anode and cathode materials balanced [11]. Therefore, we further studied  $\text{Na}@\text{Au}@\text{Cu}||\text{Na}_3\text{V}_2(\text{PO}_4)_3$  cells with different amounts of excess Na. The cells can maintain a stable capacity before the excess Na is fully consumed (Figure 4 and Figure S15). Average CE of the anode (Na) can be calculated from the cycle life using the following equation:

$$\text{CE}_{\text{avg.}, \text{Na}} = \frac{C_{\text{Na}}}{NC_{\text{NaVP}}},$$

where  $C_{\text{Na}}$  is the initial capacity of the Na anode (*i.e.*, excess Na),  $N$  is the cycle number when the capacity of the full cell starts to drop, and  $C_{\text{NaVP}}$  is the capacity of the  $\text{Na}_3\text{V}_2(\text{PO}_4)_3$  cathode. We note here that in this cycling stage the CE of the Na anode is not reflected by the CE of the cell which is actually the CE of the cathode because the anode is in excess. When a  $\sim 0.43 \text{ mAh cm}^{-2}$   $\text{Na}@\text{Au}@\text{Cu}$  anode was paired with a  $\sim 0.25 \text{ mAh cm}^{-2}$   $\text{Na}_3\text{V}_2(\text{PO}_4)_3$  cathode, which corresponds to  $\sim 0.43 \text{ mAh cm}^{-2}$  of excess Na (171.22% of  $C_{\text{NaVP}}$ ), the cell maintained its initial capacity for 260 cycles (Figure 4(a)). The average CE of Na plating/stripping was calculated to be 99.34%, which agrees well with the CE values determined using  $\text{Na}||\text{Cu}$  and  $\text{Na}@\text{Au}@\text{Cu}||\text{Au}@\text{Cu}$  half cells. When the anode excess was further lowered to 99.09% ( $\sim 0.086 \text{ mAh cm}^{-2}$  of Na paired with  $\sim 0.094 \text{ mAh cm}^{-2}$  of  $\text{Na}_3\text{V}_2(\text{PO}_4)_3$ ) and 33.84% ( $\sim 0.43 \text{ mAh cm}^{-2}$  of Na paired with  $\sim 1.27 \text{ mAh cm}^{-2}$  of  $\text{Na}_3\text{V}_2(\text{PO}_4)_3$ ), the stable-operation life was shortened to 100 and 30 cycles, giving average anode CEs of 99.09% and 98.87%, respectively (Figure 4(b), (c)). These results show that Na metal electrodes are reasonably efficient in the TEGDME electrolyte when the contact issue is solved, although the CE still needs to be improved (*e.g.*, to  $>99.9\%$ ) to better satisfy application requirements.

In conclusion, Na metal electrodes have high CE when operating in ether electrolytes but are highly irreversible in

carbonate electrolytes. Preparation and effective cycling of thin Na metal electrodes with controlled capacities is challenged by the adhesion problem between Na and Cu, which can be solved by introducing an Au interlayer. With this progress, we have reached the 99.5% level of CE, which means 400 stable cycles of the battery when the anode is 200% in excess.

**Acknowledgements** This work was supported by the U.S. National Science Foundation (CBET-1903342). Zhang Y acknowledges an exchange graduate student scholarship from the China Scholarship Council. Zhong Y acknowledges the Link Foundation Energy Fellowship. Wang H acknowledges the Sloan Research Fellowship. We thank Bingchen Deng in the Department of Electrical Engineering at Yale University for help with Au deposition on Cu. We also thank Dr. Xinxin Cao at Central South University for providing the  $\text{Na}_3\text{V}_2(\text{PO}_4)_3$  material.

**Conflict of interest** The authors declare no conflict of interest.

**Supporting information** The supporting information is available online at <http://chem.scichina.com> and <http://link.springer.com/journal/11426>. The supporting materials are published as submitted, without typesetting or editing. The responsibility for scientific accuracy and content remains entirely with the authors.

- Pan H, Hu YS, Chen L. *Energy Environ Sci*, 2013, 6: 2338–2360
- Kim SW, Seo DH, Ma X, Ceder G, Kang K. *Adv Energy Mater*, 2012, 2: 710–721
- Hwang JY, Myung ST, Sun YK. *Chem Soc Rev*, 2017, 46: 3529–3614
- Luo W, Shen F, Bommier C, Zhu H, Ji X, Hu L. *Acc Chem Res*, 2016, 49: 231–240
- Zhao Y, Adair KR, Sun X. *Energy Environ Sci*, 2018, 11: 2673–2695
- Lee B, Paek E, Mitlin D, Lee SW. *Chem Rev*, 2019, 119: 5416–5460
- Shi Q, Zhong Y, Wu M, Wang H, Wang H. *Angew Chem Int Ed*, 2018, 57: 9069–9072
- Seh ZW, Sun J, Sun Y, Cui Y. *ACS Cent Sci*, 2015, 1: 449–455
- Choudhury S, Wei S, Ozhabes Y, Gunceler D, Zachman MJ, Tu Z, Shin JH, Nath P, Agrawal A, Kourkoutis LF, Arias TA, Archer LA. *Nat Commun*, 2017, 8: 898
- Zhang Y, Zhong Y, Shi Q, Liang S, Wang H. *J Phys Chem C*, 2018,

122: 21462–21467

11 Chen S, Niu C, Lee H, Li Q, Yu L, Xu W, Zhang JG, Dufek EJ, Whittingham MS, Meng S, Xiao J, Liu J. *Joule*, 2019, 3: 1094–1105

12 Zhong Y, Xie Y, Hwang S, Wang Q, Cha JJ, Su D, Wang H. *Angew Chem Int Ed*, 2020, doi: 10.1002/anie.202004477

13 Zhang W, Wu Q, Huang J, Fan L, Shen Z, He Y, Feng Q, Zhu G, Lu Y. *Adv Mater*, 2020, 32: 2001740

14 Cohn AP, Muralidharan N, Carter R, Share K, Pint CL. *Nano Lett*, 2017, 17: 1296–1301

15 Tang S, Qiu Z, Wang XY, Gu Y, Zhang XG, Wang WW, Yan JW, Zheng MS, Dong QF, Mao BW. *Nano Energy*, 2018, 48: 101–106

16 Wang C, Wang H, Matios E, Hu X, Li W. *Adv Funct Mater*, 2018, 28: 1802282

17 Lu K, Gao S, Li G, Kaelin J, Zhang Z, Cheng Y. *ACS Mater Lett*, 2019, 1: 303–309

18 Zhu M, Wang G, Liu X, Guo B, Xu G, Huang Z, Wu M, Liu HK, Dou SX, Wu C. *Angew Chem Int Ed*, 2020, 59: 6596–6600

19 Luo W, Lin CF, Zhao O, Noked M, Zhang Y, Rubloff GW, Hu L. *Adv Energy Mater*, 2017, 7: 1601526

20 Li P, Xu T, Ding P, Deng J, Zha C, Wu Y, Wang Y, Li Y. *Energy Storage Mater*, 2018, 15: 8–13

21 Zhao Y, Goncharova LV, Zhang Q, Kaghazchi P, Sun Q, Lushington A, Wang B, Li R, Sun X. *Nano Lett*, 2017, 17: 5653–5659

22 Zhu M, Li S, Li B, Gong Y, Du Z, Yang S. *Sci Adv*, 2019, 5: eaau6264

23 Zheng X, Fu H, Hu C, Xu H, Huang Y, Wen J, Sun H, Luo W, Huang Y. *J Phys Chem Lett*, 2019, 10: 707–714

24 Chi SS, Qi XG, Hu YS, Fan LZ. *Adv Energy Mater*, 2018, 8: 1702764

25 Zhang Y, Zhong Y, Liang S, Wang B, Chen X, Wang H. *ACS Mater Lett*, 2019, 1: 254–259

26 Rodriguez R, Loeffler KE, Nathan SS, Sheavly JK, Dolocan A, Heller A, Mullins CB. *ACS Energy Lett*, 2017, 2: 2051–2057

27 Zhang XQ, Cheng XB, Chen X, Yan C, Zhang Q. *Adv Funct Mater*, 2017, 27: 1605989

28 Deng Y, Zheng J, Warren A, Yin J, Choudhury S, Biswal P, Zhang D, Archer LA. *Adv Energy Mater*, 2019, 9: 1901651

29 Fang C, Li J, Zhang M, Zhang Y, Yang F, Lee JZ, Lee MH, Alvarado J, Schroeder MA, Yang Y, Lu B, Williams N, Ceja M, Yang L, Cai M, Gu J, Xu K, Wang X, Meng YS. *Nature*, 2019, 572: 511–515

30 Gu Y, Wang WW, Li YJ, Wu QH, Tang S, Yan JW, Zheng MS, Wu DY, Fan CH, Hu WQ, Chen ZB, Fang Y, Zhang QH, Dong QF, Mao BW. *Nat Commun*, 2018, 9: 1339

31 Tang S, Zhang YY, Zhang XG, Li JT, Wang XY, Yan JW, Wu DY, Zheng MS, Dong QF, Mao BW. *Adv Mater*, 2019, 31: 1807495

32 Louli AJ, Genovese M, Weber R, Hames SG, Logan ER, Dahn JR. *J Electrochem Soc*, 2019, 166: A1291–A1299

33 Weber R, Genovese M, Louli AJ, Hames S, Martin C, Hill IG, Dahn JR. *Nat Energy*, 2019, 4: 683–689

34 Yin X, Tang W, Jung ID, Phua KC, Adams S, Lee SW, Zheng GW. *Nano Energy*, 2018, 50: 659–664